Proceedings of the XIth International Congress and Exposition
June 2-5, 2008 Orlando, Florida USA

Mechanical Strength of Pyrolytically Stripped and Functionalized Heat Treated Vapor Grown Carbon Nanofibers

Ozkan T.[a], Naraghi M.[b], Polycarpou A. A.[a], Chasiotis I.[b]
[a] University of Illinois at Urbana-Champaign, Mech. Science and Eng., Urbana, IL 61801, USA
[b] University of Illinois at Urbana-Champaign, Aerospace Engineering, Urbana, IL 61801, USA

ABSTRACT

Two grades of commercial, highly graphitic, vapor grown carbon nanofibers Pyrograf-III, that were pyrolytically stripped and heat treated, with an average outer diameter of 150 nm, were tested for their tensile strength by a MEMS-based mechanical testing platform. The applied force was measured by a surface micromachined loadcell whose deflection was extracted by digital image correlation with an accuracy of 50 nm or better. The mean strength of pyrolytically-stripped nanofibers was 2.93 GPa while the average strength of heat-treated nanofibers was 2.54 GPa. The Weibull parameters extracted from experimental data showed significant randomness in the flaw population in both types of fibers. High-resolution SEM images of matching ruptured surfaces showed purely brittle fracture, and, in some occasions, distinct partial "sword-in-sheath" type of failure. The latter was potentially due to mutual sliding of graphene planes during fiber fracture, which was attributed to the "dixie cup" structure of Pyrograf-III. This is the first experimental work that addresses the mechanics of carbon nanofibers at the individual fiber scale. To date their strength has been assumed to be similar to conventional carbon fibers.

1. Introduction

Vapor grown carbon nanofibers (VGCNFs) have the potential of significantly improving the multifunctionality of advanced composites for lightweight aerospace structures in terms of thermal and/or electrical conductivities as well as other industries that require high performance materials [1,2,3]. VGCNFs are produced by catalytic (e.g. nanoscale iron, nickel, or cobalt alloy particles) exposure of a gaseous hydrocarbons to high temperatures [4,5]. Over the length of the nanofibers, the resulting material structure is highly graphitic with an amorphous "deposited" phase on top of the graphitic phase. Morphologically, the effect of this CVD deposited layer is general thickening of the fiber and structural non-uniformities in the transverse fiber plane, depending on variations in stoichiometric conditions at different sites along the fiber axis. In general, it can be claimed that this outer annular portion of the fiber cross-section is less ordered and, perhaps more defect prone than the catalytic phase, which bears highly ordered graphite-like carbon oriented in a cone-like geometry [6].

Two different grades of highly graphitic, Pyrograf®-III, carbon nanofibers were examined in this study. The first grade, with designation PR-24 XT HHT-OX, was high-temperature heat-treated form of surface functionalized VGCNF. It has been shown that high temperature treatment creates a highly electrically conductive structure by converting the partially amorphous turbostratic layer to a graphitic one [7]. The second fiber grade was PR-24 XT PS. Post processing for these fibers differs from the previously described high temperature treatment in terms of temperature and duration. Polyaromatic hydrocarbon residues, which are by-products of the CVD process, are removed from the nanofiber surface at temperatures substantially below 2000°C. Although some analogies may be drawn from microscale carbon fibers to VGCNFs, in order to predict the effect of such treatments on the mechanical response of individual nanofibers, no direct experimental evidence exists in literature preceding this study, mostly due to the associated difficulties of experimenting at this scale.

The two material systems investigated, i.e. PR-24 XT HHT-OX and PR-24 XT PS carbon nanofibers, are 1-D nanostructures with aspect ratios of 500-1000. Taking the original formulations of Weibull [8] into account and

using the outcomes of previous studies by McCarty and Chasiotis [9,10] on quantitative failure analysis of microscale structures, it is known that if scalability is established, the results of a properly conducted Weibull analysis could be used to predict the probability of failure of larger, or smaller, self-similar structures. The primary benefit of utilizing the Weibull probability function is that it enables the assessment of material reliability as a function of load amplitude. Moreover, a properly conducted Weibull analysis also possesses the potential of associating the active flaw population with certain geometric features of the investigated material system, in our case the stacked herringbone graphitic cones, and the partially amorphous turbostratic carbon layer [5].

The goal of this work was to investigate mechanical strengths of two different grades of Pyrograf-III nanofibers. A novel MEMS-based mechanical testing method with high resolution measurements was used in the fiber strength evaluation. An effort was made to identify the principal failure modes of the two types of nanostructures, and relate those to the material microstructure. The measured fiber strengths were analyzed in terms of the Weibull cumulative function and the results are presented in this paper.

2. Experimental Method and Analysis

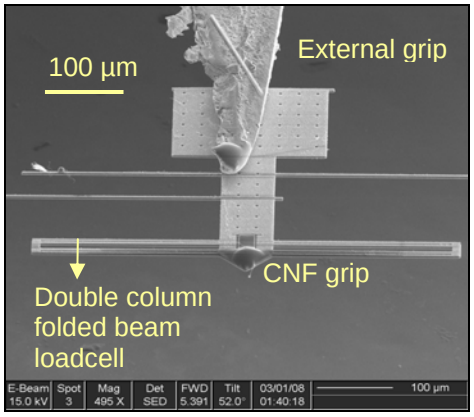

Figure 1. SEM image of a 4.5-µm thick loadcell used in experiments with carbon nanofibers.

A MEMS-based experimental setup was used in this study following the work by Naraghi *et al.* [11,12]. Individual polysilicon loadcells were picked-up by an external probe with UV curable adhesive, as in Figure 1. The spatial positioning of the loadcells was controlled with a 3D-stage under an optical microscope which was equipped with a high resolution CCD camera. VGCNFs were treated with distilled water to remove agglomerates and isolate individual nanofibers by a sharp tungsten probe. Various fiber disentanglement techniques, such as ultrasonication and high shear mixing, were attempted to break the agglomerates but these were finally abandoned due to substantial reduction in individual fiber length. A controlled amount of UV-curable epoxy adhesive was deployed on the crosshead of the polysilicon loadcell to mount each fiber, while the free end of the carbon nanofiber was fixed to a moving platform.

The actual stiffnesses of the 4.5-µm and 6-µm thick folded beam double column loadcells were calibrated experimentally. Microscale glass beads of known volume and density were hung on the loadcell and their calculated weights were plotted with respect to the measured loadcell deflection (by means of DIC), see Figures 2(a,b). Then, the loadcell stiffness was extracted from the slope of the least square fit, Figure 2(c). The true stiffness of the 6-µm thick folded beam loadcells was 1.59 N/m, which was about 4 times smaller than the nominal value, computed by using the loadcell dimensions. On the other hand, the geometry definition of the 4.5 µm thick loadcells (after fabrication) was much more accurate and their true stiffness was 4.74 N/m, which was less than 5% smaller than the expected stiffness. Both ends of the ruptured carbon nanofibers were imaged by an SEM at 200kX to measure the inner and outer fiber diameter and investigate the mode of failure. Although it was possible to determine the outer radius accurately, determining the inner radius of the hollow cylindrical structures was not always possible due to e-beam induced motion (charging) of the ruptured fiber ends, and the difficulty to position the fiber cross-section normal to the SEM detector.

The analysis of fiber strengths was done by the 2-parameter Weibull cumulative density function for uniform tension. The location parameter in the original 3-parameter formulation [10] was assumed to be zero so that a conservative description of strength is obtained. Then, the Weibull probability function takes the form:

$$P_f(\sigma) = 1 - \exp\left(-\left(\frac{\sigma}{\sigma_0}\right)^m\right) \tag{1}$$

where the parameters m and σ_0 are "material constants". The stress, σ, is the applied stress which results in probability of failure, $P_f(\sigma)$. The shape parameter (or Weibull modulus) m, indicates the degree of scatter in the strength data. The stress level at which the probability of failure becomes 63.2% is the characteristic strength. This value is useful for comparison purposes of the different grades of Pyrograf III.

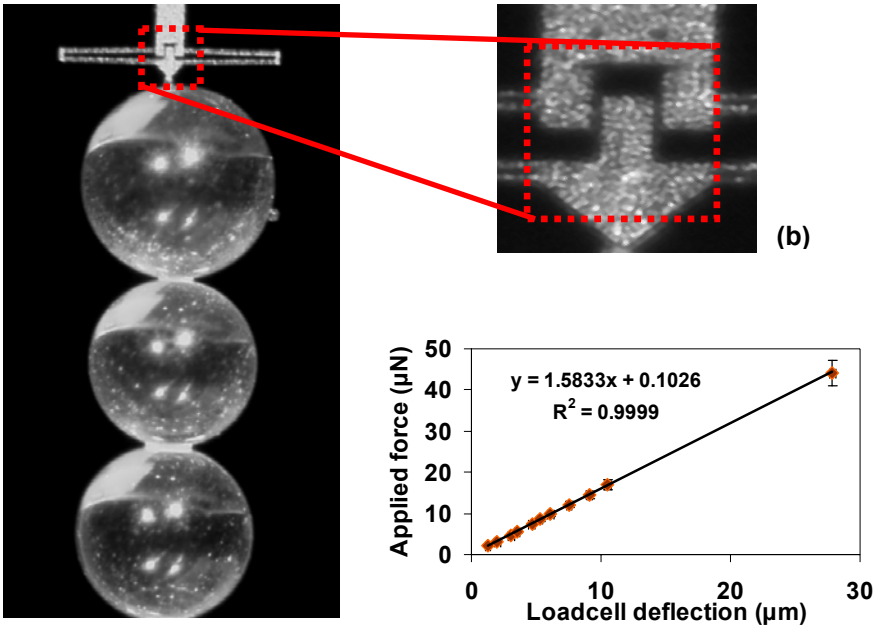

Figure 2. (a) Calibration of a loadcell as imaged by a macro camera objective lens, **(b)** detail of the loadcell grip deflection during calibration, **(c)** force-deflection curve for a 6-µm thick loadcell.

By taking twice the natural logarithm of both sides in equation (1), linear regression analysis could be applied to find the Weibull modulus, m, and the scale parameter:

$$\ln\left(\ln\left(\frac{1}{1-P_{f\ i}}\right)\right) = m\ln(\sigma_i - \sigma_u) - m\ln\sigma_0 \tag{2}$$

For the relatively small sample sizes used in this work, Bernard's method of probability estimation is assumed [13], so that

$$P_{f\,i}(\sigma) = \frac{i - 0.3}{n + 0.4} \tag{3}$$

where n is the total number of data points and i is the ordinal rank of a single datum point.

Because of the small number of samples, the maximum likelihood method was also applied to identify the best description of our data sets [14]. In order to calculate the parameters of the optimum likelihood function which

provides the best fit for the data set at hand, a system of equations can be generated by setting the partial derivatives of the likelihood function with respect to the sought parameters m and σ_C equal to zero. Hence, the following system of coupled equations is obtained, which is solved numerically to determine $\hat{m}$ and $\hat{\sigma}_C$, i.e. the maximum likelihood estimates of the Weibull modulus and the characteristic strength respectively:

$$\hat{\sigma}_C = \left[\left(\frac{1}{n} \right) \sum_{i=1}^{n} \sigma_i^{\hat{m}} \right]^{1/\hat{m}} \tag{4}$$

$$\hat{m} = \frac{n}{\left(\frac{1}{\hat{\sigma}_C} \right)^{\hat{m}} \sum_{i=1}^{n} \sigma_i^{\hat{m}} \ln \sigma_i - \sum_{i=1}^{n} \ln \sigma_i} \tag{5}$$

3. Results and Discussion

The average nominal strength of pyrolytically stripped nanofibers based on their outer fiber diameter was 2.93 GPa compared to the average strength of heat-treated functionalized nanofibers, which was measured to be 2.54 GPa. The Weibull parameters computed for the two data sets from Figures 3(a,b) are shown in Table 1. In both fiber types the Weibull modulus was relatively small indicating a broad spectrum of flaws. The maximum likelihood analysis provided better fitting of the probability of failure vs. fiber strength data, potentially due to the small number of data that could not be described adequately by the probability estimator in Equation (3). It is characteristic that the strength of pyrolytically stripped nanofibers was consistently about 20% higher than that of heat-treated and functionalized nanofibers. Although it is expected that the heat-treated nanofibers will have smaller and less broad flaw populations that the pyrolytically stripped ones, the process of surface functionalization generates additional surface flaws that potentially decreased the average fiber strength but reduced the scatter in flaw sizes. The latter argument is validated by the 50% large Weibull modulus of heat treated nanofibers which points to a tighter distribution of flaws.

Table 1. Weibull parameters based on maximum likelihood and linear regression estimation methods

Weibull parameter	Maximum likelihood function		Linear regression analysis	
	PR-24 XT HHT-OX	PR-24 XT PS	PR-24 XT HHT-OX	PR-24 XT PS
Weibull modulus, m	3.59	2.42	3.43	1.94
Characteristic strength, σ_C, (GPa)	2.82	3.31	2.83	3.38

A contributing factor to the scatter in fiber strength values is the fact that these parameters were extracted taking into account the nominal fiber strength, without accounting for variations in the inner fiber diameter. This is partly justified because the hollow structure of VGCNFs is not taken into account when they are integrated in polymer nanocomposites. Instead, their nominal strength values may be used in micromechanics models. Of course, this is not true if polymer matrix is infiltrated into the hollow nanofiber. Additionally, two distinct types of HHT-OX nanofibers were tested: Those with uniform cross-section, and fibers with fluctuating (rippled) cross-section. In the second type, the fiber diameter was taken as the one at the fracture site. It must also be noted that the two

types of fibers (rippled and uniform) failed at similar nominal stress values, so no particular biasing of the data has occurred. Finally, in both methods for parameter estimation, PS fibers were quite stronger than HHT-OX fibers. Therefore it can be argued that although high temperature heat treating increases the degree of graphitization and, thus, enhances their thermal and electrical transport properties, this functional improvement is achieved at the expense of tensile strength, when combined with surface treatments.

Based on the effective strength values obtained by using the outer fiber diameter, no distinct scaling effect could be identified between the experimentally determined fiber tensile strengths and the nominal outer diameter. This fact might imply that the turbostratic layer could be the most influential parameter (i.e. location of critical flaw population) in defining the tensile strength of VGCNFs. For the carbon nanofibers whose detailed cross-sectional pictures could be taken at their rupture surface, the true strength calculated using the annular cross-section was as high as 8.7 GPa, indicating that the intrinsic strength of vapor grown carbon fibers might indeed converge towards those of graphite microfibers.

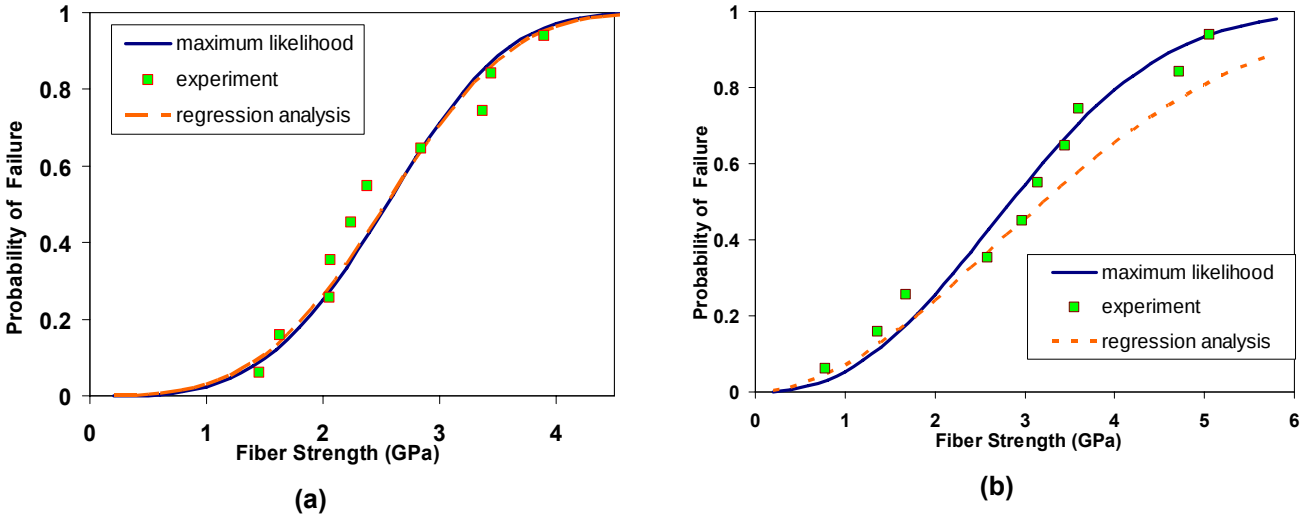

Figure 3. Weibull probability of failure vs. applied uniform stress for **(a)** PR-24 XT HHT-OX and **(b)** PR-24 XT PS carbon nanofibers.

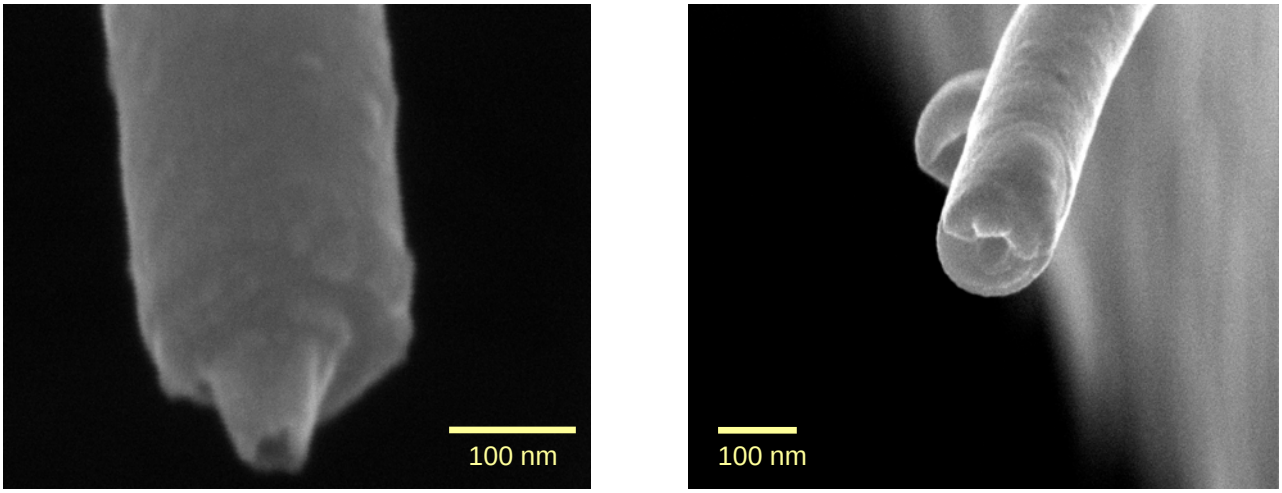

Figure 4. Rupture surfaces of hollow PR-24 XT PS VGCNFs. The “sword-in-sheath” failure seen in the left figure is associated with the “dixxie cup” structure of the fibers.

Mutual sliding of graphene planes, or the so-called “sword in sheath” type failure, occurred in parallel with brittle fracture of the fiber outer shell, where failure was potentially initiated for nanofibers of both grades. Direct visual evidence of this argument is provided in Figure 4, where a “sword in sheath” morphology was clear in the rupture surfaces.

4. Conclusions

The strength of individual VGCNFs PR-24 XT PS and PR-24 XT HHT-OX was measured for the first time and was analyzed in terms of the Weibull cumulative distribution function. The characteristic strength, obtained by the maximum likelihood function, for PR-24 XT PS was 20% higher than that of PR-24 XT HHT-OX which indicates that heat treatment, when combined with surface functionalization does not improve on the mechanical performance of the nanofibers. On the other hand it was shown that heat-treatment does improve of the spectrum of flaw distributions in the nanofibers decreasing the scatter in tensile strength values by as much as 50%. Post-mortem SEM imaging showed that fiber failure is purely brittle in the amorphous outer fiber turbostratic layer, followed by “sword in sheath” failure of the graphitic inner annulus.

5. Acknowledgements

The authors gratefully acknowledge the support by the Air Force Office of Scientific Research (AFOSR) through Grant FA9550-06-1-0140 with Dr. B.L. Lee as the program manager. The authors would like to thank Dr. H. Kahn at CASE for the fabrication of the MEMS loadcells and Dr. M. Marshall at the Materials Research Laboratory of UIUC for his helpful suggestions regarding SEM imaging of nanofibers.

6. References

[1] Mai, Y. W. Yu, Z.Z., Polymer Nanocomposites, First ed., Woodhead Publishing Ltd., Cambridge, UK, 2006

[2] Finegan, I.C. et al. “Surface treatments for improving the mechanical properties of carbon nanofiber/thermoplastic composites”, Journal of Materials Science 38, pp. 3485-3490, 2003

[3] Burton, D. J. et al. “Influence of carbon nanofiber surface characteristics on composite properties”, Proc. of 46th International SAMPE Symposium, pp. 647-657, 2001

[4] Suresh, G.A., Processing and Properties of Nanocomposites, First ed., World Scientific Publishing Co. Pte. Ltd., Singapore, 2007

[5] Baker, R. T. K. “Synthesis, Properties and Applications of Graphite Nanofibers”, WTEC Workshop Report on R&D Status and Trends in Nanoparticles, Nanostructured Materials, and Nanodevices in the United States, Proceedings, 1997, available online at http://www.wtec.org/loyola/nano/US.Review/09_03.htm

[6] Lake, M. et al. “Carbon Nanofiber Polymer Composites: Electrical and Mechanical Properties”, Proc. of 47th International SAMPE Symposium, pp. 1794-1800, 2002

[7] Burchell, T.D., Carbon Materials for Advanced Technologies, First ed., Elsevier Science Ltd., Oxford, UK,1999

[8] Hallinan, A. J. “A Review of the Weibull Distribution”, Journal of Quality Technology 25 pp. 85-93, 1993

[9] McCarty, A. Chasiotis, I. "Description of Brittle Failure of Non-uniform MEMS Geometries", Thin Solid Films 515 pp. 3267-3276, 2007

[10] McCarty, A. Chasiotis, I. “Quantitative Failure Analysis for MEMS Materials with Multiple Active Flaw Populations” Proc. of Soc. Exper. Mech. 214 pp. 1103-1108, 2005.

[11] Naraghi, M., Chasiotis, I., Dzenis, Y., Wen, Y., Kahn, H., “Novel Method for Mechanical Characterization of Polymeric Nanofibers”, Review of Scientific Instruments 78 pp. 085108, 2007

[12] Naraghi, M., Chasiotis, I., Dzenis, Y., Wen, Y., Kahn, H., “Mechanical deformation and failure of electrospun polyacrylonitrile nanofibers as a function of strain rate”, Applied Physics Letters 91 pp. 151901, 2007

[13] Sullivan, J. D. Lauson, P. H. “Experimental probability estimators for Weibull plots”, Mat. Sci. Letters 5 pp. 1245-1247, 1986

[14] Evans, M. et al., Statistical Distributions, Second ed., John Wiley & Sons Inc., New York, NY, 1993